A semi-Lagrangian particle level set finite element method for interface problems

R. Bermejo

Department of Applied Mathematics
Universidad Politecnica de Madrid

Rome-2011

Outline

Introduction. Definition of the level set method

- The level set method is a front capturing technique to calculate the motion of fluid interfaces, as well as curves or surfaces whose speeds depend on local curvatures.

- The technique uses a fixed (Eulerian) mesh and finds the front as the zero level set (moving with time) of the signed distance function to the interface.

Basic bibliography

- S. Osher and J.A. Sethian, *Fronts propagating with curvature dependent speed: algorithms based on Hamilton-Jacobi formulations.* J. Comput. Phys. **79** (1988), pp. 12-49.
- J. A. Sethian, *Level Set Methods and Front Marching Methods.* Cambridge University Press (1999).
- S. Osher and R. Fedkiw, *Level Set Methods and Dynamic Implicit Surfaces.* Springer-Verlag. Berlin, Heidelberg (2002).

Level set formulation

Let $D \subset \mathbb{R}^d$ ($d = 2$ or 3) be a bounded domain with boundary ∂D. For simplicity, assume D is composed of two subdomains, say, D_1 and D_2 (possibly multiconnected) with boundaries ∂D_i $(1 \leq i \leq 2)$ and Γ_0, such that

$$D = D_1 \cup D_2 \cup \Gamma_0.$$

- Γ_0 is a $d-1$ manifold separating the domains D_1 and D_2 and undergoing a time dependent motion : $\Gamma_0(t)$, $t \in [0, T]$.
- $\Gamma_0(t)$ is called interface.
- At $t = 0$, $\Gamma_0(0)$ is known.
- Let $u(t) : D \to \mathbb{R}$,
-
$$\Gamma_0(t) := \{x \in D : u(x,t) = 0\}.$$

Level set formulation

- $\Gamma_0(t)$ is the zero level set of u.
- For many purposes is good to choose u as

$$u(x,t) = \pm \min_{y \in \Gamma_0(t)} |x - y|, \quad x \in D, \tag{1}$$

- $|x - y|$ denotes the Euclidean distance.
- Note that on the levels set $u(x,t) = C$,
  $$\frac{Du}{Dt} = \frac{\partial u}{\partial t} + v \cdot \nabla u = 0,$$
- $v(x,t) = \frac{dx}{dt}$ is a velocity field defined in D,
- when $x \in \Gamma_0(t)$, $v(x,t)$ is the velocity of the points of the interface.

Level set formulation

- Characterization of $u(x,t)$
  (1) On any level set $u(x,t) = C$: The initial value problem.

$$\begin{cases} \dfrac{Du}{Dt} = \dfrac{\partial u}{\partial t} + v \cdot \nabla u = 0 \text{ in } \ D \times (0, T], \\ u(x,0) = \pm \min_{y \in \Gamma_0(0)} |x - y|, \quad x \in D, \end{cases} \tag{2a}$$

  (2) The distance property.

$$|\nabla u| = 1, \tag{2b}$$

  and
  (3)

$$u(x,t) \begin{cases} > 0 \quad \text{if} \ \ x \in D_1, \\ = 0 \ \text{ if } x \in \Gamma_0(t), \\ < 0 \ \text{ if } \ x \in D_2. \end{cases} \tag{2c}$$

Level set formulation

- Nice features of the level set method
  Easy to calculate the geometr4ic quantities
  - the normal to the level set $U = C$

$$\mathbf{n} = \frac{\nabla u}{|\nabla u|}, \tag{3a}$$

  - the curvature

$$\kappa = -\nabla \cdot \mathbf{n}, \tag{3b}$$

  - the integral

$$|D_2| = \int_D H(-u)dx, \tag{3c}$$

  - the graph of Heaviside

$$H(u) = \begin{cases} 1 \text{ if } u > 0, \\ [0,1] \text{ if } u = 0, \\ 0 \text{ if } u < 0. \end{cases} \tag{3d}$$

Outline

Reinitialization

- Problems with this approach
  - The numerical solution of the linear advection equation looses its distance character.
  - Due to numerical errors, the conservation of volume property (also known as mass conservation) is also lost.
  - After few time steps, u may become irregular or flat in some regions of the domain.

- Remedies
  - Reinitialization or redistancing.
    Replace $u(x, t_n)$ by a signed distance function $d(x, t_n)$ that has the same zero level set and better regularity properties, then set

    $$u(x, t_n) = d(x, t_n),$$

    and go to solve equation (2a) to calculate $u(x, t_{n+1})$.

Reinitialization

Procedures to reinitialization

- Direct: geometrical or optimization
- Fast marching
- Hyperbolic PDE
- We use a mixed procedure: Direct (near) Hyperbolic (far).

- Basic references on hyperbolic reinitialization:
  - M. Sussman, P. Smereka and S. Osher, *A level set approach for computing solutions to incompressible two-phase flow.* J. Comput. Phys. **114** (1994), pp. 146-159.
  - M. Sussman and E. Fatemi, *An efficient interface preserving level set redistancing algorithm and its applications to interfacial incompressible fluid flow.* SIAM J. Sci. Comput. **20** (1999), pp. 1165-1191.

Reinitialization

- M. Sussman, P. Smereka and S. Osher Reinitialization procedure:
  - For $d : D \times [0, T^*] \to \mathbb{R}$ solve up to reach the steady state the first order nonlinear hyperbolic problem

$$\begin{cases} \dfrac{\partial d(x,\tau)}{\partial \tau} + w \cdot \nabla d = sign(u(x,t)) \text{ in } D \times (0, T^*], \\ d(x,0) = u(x,t), \end{cases} \tag{4a}$$

$$w = sign(u(x.t))\frac{\nabla d}{|\nabla d|} = sign(u(x.t))\mathbf{n}. \tag{4b}$$

  - Note that when $\dfrac{\partial d(x,\tau)}{d\tau} = 0, \quad |\nabla d| = 1$!!!!Distance!!!!
  - Note that $w = 0$ on $\Gamma_0(t)$

Reinitialization

Solution to equation (4a)

- (Far field solution)

$$In\ D_1, \quad d(x,\tau) = \begin{cases} \tau + u(X_w(x,\tau;0),t) & \text{if } \tau \le t^*, \\ t^* & \text{if } \tau > t^*, \end{cases} \tag{5a}$$

t^* being the shortest distance from x to the zero level set,

$$In\ D_2, \quad d(x,\tau) = \begin{cases} -\tau + u(X_w(x,\tau;0),t) & \text{if } \tau \le t^*, \\ -t^* & \text{if } \tau > t^*. \end{cases} \tag{5b}$$

- Near field solution
  Since $u \in C^2$ in D_1 and D_2, for τ small enough, in a neighborhood of $\Gamma_0(t)$

$$d(x_0 \pm \tau \mathbf{n}(x_0)) = \pm\tau, \quad x_0 \in \Gamma_0(t) \tag{6}$$

Reinitialization

- Equation of the characteristics

$$\begin{cases} \dfrac{dX_w(x,s,\tau)}{d\tau} = w(X_w(x,s,\tau),\tau) \text{ in } D \times (0,T^*], \\ \\ X_w(x,s;s) = x. \end{cases} \quad (7)$$

- The new level set function at time t is

$$u(x,t)) = d(x,\tau^*) \; in \; D \quad (8)$$

- Remark. Due to numerical errors the solution (8) does not satisfy yet the mass conservation property.
- Particle Level set (PLS)

- Step 1: Quasi-monotone semi-Lagrangian scheme (QMSL) to calculate u_h^n as an approximation to

$$\begin{cases} \dfrac{Du}{Dt} = \dfrac{\partial u}{\partial t} + v \cdot \nabla u = 0 \text{ in } D \times (0, T], \\ u(x, 0) = \pm \min_{y \in \Gamma_0(0)} |x - y|, \quad x \in D, \end{cases} \tag{9}$$

- Step 2: Apply the PLS method to correct u_h^n
- Step 3 Apply the QMSL scheme to calculate the numerical solution of the far field reinitialization.

$$In\ D_1, \quad d(x, \tau) = \begin{cases} \tau + u(X_w(x, \tau; 0), t) \text{ if } \tau \leq t^*, \\ t^* \text{ if } \tau > t^*, \end{cases} \tag{10}$$

$$In\ D_2, \quad d(x, \tau) = \begin{cases} -\tau + u(X_w(x, \tau; 0), t) \text{ if } \tau \leq t^*, \\ -t^* \text{ if } \tau > t^*. \end{cases} \tag{11}$$

Numerical method

- Space discretization: Finite elements P_1-iso P_2
- Partitions: D_H and D_h
- Finite element spaces associated to the partitions

$$V_h := \{v_h \in C^0(\overline{D}) : v_h\,|_{T_j} \in P_1(T_j),\ 1 \leq j \leq NE2\},$$
$$V_H := \{w_H \in C^0(\overline{D}) : w_H\,|_{T_k} \in P_2(T_k),\ 1 \leq k \leq NE1\}, \tag{12}$$

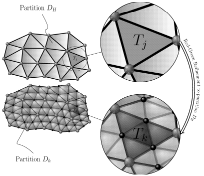

Outline

Numerical method: QMSL level set equation

$$\frac{Du}{Dt} = 0, \; t_{n-1} \leq t \leq t_n, \tag{13}$$

implies that

$$u(x, t_n) = u(X(x, t_n; t_{n-1}), t_{n-1}), \tag{14}$$

$$\begin{cases} \dfrac{dX(x, t_n; t)}{dt} = v(X(x, t_n; t), t), \quad t_{n-1} \leq t < t_n, \\ \\ X(x, t_n, t_n) = x. \end{cases} \tag{15}$$

Assuming that $v \in L^\infty(0, T; W^{1,\infty}(D)^d)$,

$$X(x, t_n; t) = x - \int_t^{t_n} v(X(x, t_n; \tau), \tau) d\tau. \tag{16}$$

Numerical method: QMSL level set equation

$$u_h^n(x_i) = u_h^{n-1}(X_h(x_i, t_n; t_{n-1})). \tag{17}$$

where $X_h(x_i, t_n; t_{n-1})$ denotes the calculated numerical approximation to the exact $X(x_i, t_n; t_{n-1})$

- At time t_n, we calculate the values $u_h^n(x_i) := U_i^n$, $1 \leq i \leq NN$, by the formula

$$\boxed{U_i^n = (1 - \beta_i^{n-1}) I_h u_h^{n-1}(X_h(x_i, t_n; t_{n-1})) + \beta_i^{n-1} I_H u_h^{n-1}(X_h(x_i, t_n; t_{n-1}))} \tag{18}$$

- $I_h : C(\overline{D}) \rightarrow V_h$ and $I_H : C(\overline{D}) \rightarrow V_H$ interpolation operators.

$$I_h u_h^{n-1}(X_h(x_i, t_n; t_{n-1})) = \sum_{i=1}^{NN} U_i^{n-1} \psi_i(X_h(x_i, t_n; t_{n-1})), \tag{19}$$

$$I_H u_h^{n-1}(X_h(x_i, t_n; t_{n-1})) = \sum_{i=1}^{NN} U_i^{n-1} \overline{\psi}_i(X_h(x_i, t_n; t_{n-1})). \tag{20}$$

Numerical method: QMSL level set equation

- Calculation of the limiting coefficients β_i^{n-1}
  $\overline{T}_k \in D_H$, containing $X_h(x_i, t_{n+1}; t_{n-1})$, then calculate

$$\begin{cases} U^+ = \max u_h^{n-1} \mid_{Nodes(\overline{T}_k)} \text{ and } U^- = \min u_h^{n-1} \mid_{Nodes(\overline{T}_k)}, \\ Q^\pm = U^\pm - I_h u_h^{n-1}(X_h(x_i, t_n; t_{n-1})), \\ P = I_H u_h^{n-1}(X_h(x_i, t_n; t_{n-1})) - I_h u_h^{n-1}(X_h(x_i, t_n; t_{n-1})), \end{cases} \tag{21}$$

$$\begin{cases} \text{If } P > 0, \quad \beta_i^{n-1} = \min\left(1, \dfrac{Q^+}{P}\right), \\ \text{else if } P < 0, \; \beta_i^{n-1} = \min\left(1, \dfrac{Q^-}{P}\right), \\ \text{else if } P = 0, \quad \beta_i^{n-1} = 1. \end{cases} \tag{22}$$

Numerical method: QMSL level set equation

- Summarizing

$$U_i^n = \begin{cases} U^+ \text{ if } I_H u_h^{n-1}(X_h(x_i, t_n; t_{n-1})) > U^+, \\ U^- \text{ if } I_H u_h^{n-1}(X_h(x_i, t_n; t_{n-1})) < U^-, \\ I_H u_h^{n-1}(X_h(x_i, t_n; t_{n-1})) \text{ otherwise.} \end{cases} \quad (23)$$

Finally, we set:

$$u_h^n(x) = \sum_{i=1}^{NN} U_i^n \psi_i(x). \quad (24)$$

Outline

Numerical method: PLS method

- Distribute randomly n_p massless particles in a band Σ_β of radius β around the zero level set

$$\Sigma_\beta = \{x \in D : 0 \leq \min_{y \in \Gamma_{h0}(t)} |x - y| \leq \beta h\}.$$

- For each particle and time t_n

$$\text{Position} \quad \left\{ \begin{array}{l} \dfrac{dx_p(t)}{dt} = v(x_p(t), t), \quad t_{n-1} < t \leq t_n, \\ \\ x_p(t_{n-1}) = x_p^{n-1} \text{ is a datum,} \end{array} \right. \tag{25}$$

$$\text{radius} \quad r_p^n = \left\{ \begin{array}{l} r_{\max} \quad \text{if} \quad s_p^n u_h^n(x_p^n) > r_{\max}, \\ \\ s_p^n u_h^n(x_p^n) \quad \text{if} \quad r_{\min} \leq s_p^n u_h^n(x_p^n) < r_{\max}, \\ \\ r_{\min} \quad \text{otherwise,} \end{array} \right. \tag{26}$$

where $s_p^n = sign u_h^n(x_p^n)$, i.e., $s_p^n = 1$ if $u_h^n(x_p^n) > 0$, etc.

Numerical method: PLS method

- $r_{min} \leq r_p \leq r_{max}, \quad r_{min} = 0.01h, \quad r_{max} = 0.05h$
- Escaped particle: An escaped particle is the one that crosses the interface by a distance larger than its radius r_p^n
- Level set of an escaped particle

$$u_{hp}^n(x) = s_p^n(r_p^n - \left|x - x_p^n\right|). \tag{27}$$

$u_{hp}^n(x)$ is locally computed at the vertices of the element in which is located.

- E_p^+ and E_p^+ be the set of escaped positive and negative particles

$$u_h^+(x) = \max_{p \in E^+} \left(u_{hp}^n(x), u_h^+(x)\right), \text{ for } u_{hp}^n(x) > 0 \tag{28}$$

$$u_h^-(x) = \min_{p \in E^-} \left(u_{hp}^n(x), u_h^-(x)\right) \text{ for } u_{hp}^n(x) < 0. \tag{29}$$

u_h^+ and u_h^- in the above two equations are initialized with u_h^n

Numerical method: PLS method

- Finally, the corrected level set function is

$$u_h^n(x) = \begin{cases} u_h^+(x) & \text{if} \quad \left|u_h^+(x)\right| \leq \left|u_h^-(x)\right|, \\ u_h^-(x) & \text{if} \quad \left|u_h^+(x)\right| > \left|u_h^-(x)\right|. \end{cases} \tag{30}$$

- Radii adjusment: the particles which remain escaped have their radius set to r_{min}.

Numerical method: PLS method

- **PLS algorithm**

  Choose the parameters β, n_p, $r_{\min}$ and $r_{\max}$

  (1) At $t = 0$:

  (1.1) Distribute randomly n_p particles in a band of radius βh around the zero level set $u_h(x, 0) = 0$.

  (1.2) For each particle p find its position x_p^0, calculate its radius r_p^0 using and identify whether is $+$ or $-$.

  (2) At t_n, assuming u_h^n is known:

  (2.1) For each particle p calculate $x_p^n$and r_p^n, and define the sets E^+ and E^-.

  (2.2) (Quantify the error) For each particle p calculate $u_{hp}^n(x)$ at the vertices of the element where is located.

  (2.3) (Error correction) Calculate the new $u_h^n(x)$.

Outline

Numerical method: QMSL for reinitialization

- Near field reinitialization

$$\Sigma_{\Gamma_{h0}(t_n)} = \{\bigcup_k T_k,\ \ T_k \in D_h : T_k \cap \Gamma_{h0}(t_n) \neq \emptyset\}.$$

Figure 2 shows graphically a piece of $\Sigma_{\Gamma_{h0}(t_n)}$.

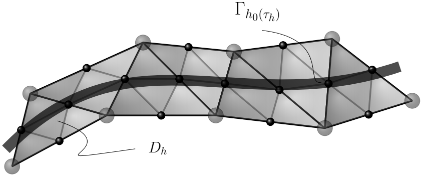

Figure: A piece of the zero level set at time t_n

- D_l the distance of nodes x_l of $\Sigma_{\Gamma_{h0}(t_n)}$ to $\Gamma_{h0}(t_n)$ is calculated by geometric or optimization procedures.

Numerical method: QMSL for reinitialization

- Far field reinitialization
  - Define $\Omega_1 := D - (D_2 \cup \Sigma_{\Gamma_{h0}(t_n)})$ and $\Omega_2 := D - (D_1 \cup \Sigma_{\Gamma_{h0}(t_n)})$
  - Write the equation to d as

$$d(x,\tau_m) = d(X_w(x,\tau_m;\tau_{m-1}),\tau_{m-1}) + \begin{cases} \Delta\tau & \text{if } x \in \Omega_1, \\ -\Delta\tau & \text{if } x \in \Omega_2, \end{cases} , \quad (31)$$

    with the initial condition $d(x,\tau_0) = u_h^n(x)$
  - Solve (31) by finite elements-QMSL method to get

$$\begin{cases} D_i^m = \overline{D}_i^{m-1} + \Delta\tau & \text{if } x_i \in \Omega_1, \\ D_i^m = \overline{D}_i^{m-1} - \Delta\tau & \text{if } x_i \in \Omega_2, \\ D_i^m = D_i & \text{if } x_i \in \Sigma_{\Gamma_{h0}(t_n)}. \end{cases} \quad (32)$$

    When $m = m_1$, the new level set function at time t_n is then

$$u_h^n(x) = d_h^{m_1}(x). \quad (33)$$

Analysis: Stability in the L^∞-norm

- Maximum mesh-dependent norm:

$$\|v\|_{h,\infty} = \max_j |v(x_i)|, \quad v \in C(\overline{D}),$$

- Equivalence of norms

$$\|v_h\|_{h,\infty} \leq \|v_h\|_{L^\infty(D)} \leq \|v_h\|_{h,\infty}$$

Lemma

Let $\Delta t \in (0, \Delta t_0)$ and $h \in (0, h_0)$, $0 < \Delta t_0 < 1$ and $0 < h_0 < 1$. Then for any $t_n \in [0, T]$ the solution obtained by QMSL satisfies

$$\|u_h^n\|_{L^\infty(D)} \leq \left\|u^0\right\|_{L^\infty(D)}.$$

- Idea of the proof: Let k be an index such that $\left\|u_h^{n-1}\right\|_{h,\infty} = \left|U_k^{n-1}\right|$, then by construction it follows that there is an index l such that

$$\|u_h^n\|_{h,\infty} = |U_l^n| \leq \left|U_k^{n-1}\right|,$$

Analysis: Error estimates

- $\overline{u}_h^n(x)$ QMSL level set solution and $u_h^n(x)$= QMSL reinitialization $\circ$ PLS($\overline{u}_h^n(x)$)
- At time t_n:

$$e^n(x) = u^n(x) - u_h^n(x) \text{ and } \overline{e}^n(x) = u^n(x) - \overline{u}_h^n(x).$$

- Ansatz

$$\|e^n\|_{h,\infty} \leq \gamma^n \left\|\overline{e}^n\right\|_{h,\infty}, \; 0 < \gamma^n \leq 1. \tag{34}$$

- Note the β_i^{n-1} are the largest possible values that minimize $\left\|u^n - \overline{u}_h^n\right\|_{h,\infty}$ while $\overline{u}_h^n$ satisfies the maximum principle locally.
- Let $0 \leq \alpha_i^{n-1} \leq \beta_i^{n-1} \leq 1$, and

$$\overline{U}_i^{*n} = \left(1 - \alpha_i^{n-1}\right) I_h u_h^{n-1}(X(x_i, t_n; t_{n-1})) + \alpha_i^{n-1} I_H u_h^{n-1}(X(x_i, t_n; t_{n-1})),$$

- $$\left\|u^n - \overline{u}_h^n\right\|_{h,\infty} \leq \left\|u^n - \overline{u}_h^{*n}\right\|_{h,\infty}.$$

Analysis: Error estimates

- $\widetilde{\beta}_i^{n-1} \longrightarrow u^{n-1}(X(x, t_n; t_{n-1}))$
- $\overline{\beta}_i^{n-1} \longrightarrow u^{n-1}(X(x, t_n; t_{n-1})) - u_h^{n-1}(X(x, t_n; t_{n-1}))$
- $$\alpha_i^{n-1} = \min(\widetilde{\beta}_i^{n-1}, \overline{\beta}_i^{n-1}, \beta_i^{n-1}),$$
- Error estimate with exact departure points

Theorem

Assume that for all n the ansatz (34) holds and $u^n(x) \in W^{r+1,\infty}(D)$, $r \geq 0$. *Then there exist positive constants* C_4 *and* K, C_4 *being independent of* Δt *and* h, *and* $0 < K \leq 1$, *such that for* $p = \min(2, r+1)$ *and* $q = \min(3, r+1)$

$$\|e^n\|_{h,\infty} \leq \frac{Kt_n}{\Delta t} \min\left(1, \frac{\Delta t \, \|v\|_{L^\infty((0,t_n)\times D)^d}}{h}\right) \times$$

$$C_4 \left[\max_{i,n}(1-\alpha_i^{n-1})h^p + h^q\right] |u|_{l^\infty(0,t_n;W^{r+1,\infty}(D))} \, . \tag{35}$$

Analysis: Error estimates

- Error estimates with non exact departure points

Theorem

Let the assumptions of Theorem 1 hold. Then, when the departure points $X_h(x, t_n; t_{n-1})$ are calculated by a single step method of order $k \geq 2$, we have that

$$\|e^n\|_{h,\infty} \leq \frac{Kt_n}{\Delta t} \min\left(1, \frac{\Delta t \, \|v\|_{L^\infty((0,t_n)\times D)^d}}{h}\right) \times$$
$$\left[\max_n \max_i (1 - \alpha_i^{n-1}) h^p + h^q\right] |u|_{l^\infty(0,t_n;W^{r+1,\infty}(D))} + \tag{36}$$
$$C_5 K t_n \left(\|v - v_h\|_{l^\infty(0,t_n;L^\infty(D)^d)} + \Delta t^k \left\|D_t^k v\right\|_{L^\infty(0,t_n;L^\infty(D)^d)}\right).$$

Outline

- Numerical tests: Zalesak slotted circle

$$\begin{cases} \dfrac{\partial u}{\partial t} + v \cdot \nabla u = 0 \ \text{ in } \ (0,1)^2 \times (0,T], \\ \\ u(x,0) = u^0(x) = \pm \min_{y \in \Gamma(0)} |x - y| \,. \end{cases} \tag{37}$$

$\Gamma_0(0)$ is the zero level set at time $t = 0$ and is represented by the boundary of a circle of radius 0.15 centered at $(0.5, 0.75)$, with a slot of depth 0.25 and width 0.05. The stationary velocity field v is given by

$$v_1(x_{1,} x_2) = 0.5 - x_2, \;\; v_2(x_1, x_2) = x_1 - 0.5,$$

Numerical tests: Zalesak slotted circle

- Parameters
  - Meshes: $M_1 = 50 \times 50$, $M_2 = 100 \times 100$, $M_3 = 200 \times 200$.
  - Δt: $\Delta t_1 = 5.0 \cdot 10^{-2}$, $\Delta t_2 = 1.0 \cdot 10^{-2}$, $\Delta t_1 = 5.0 \cdot 10^{-3}$.
  - (PLS): $r_{min} = 0.01h$, $r_{max} = 0.05h$, $n_p = 1.5 \cdot 10^4$, $\beta = 1.5$.
  - Reinitialization: every time step, $m_1 = 4$, $\Delta\tau = \frac{\Delta t}{10}$
  - $$A_{loss} = \int_D (H(u) - H(u_h))\, dx.$$

Meshes	Area loss	l^∞	L^1-order	l^∞-order
M_1	$3.92 \cdot 10^{-3}$	$7.62 \cdot 10^{-2}$	NA	NA
M_2	$1.88 \cdot 10^{-3}$	$2.44 \cdot 10^{-2}$	1.06	1.55
M_3	$7.13 \cdot 10^{-4}$	$2.40 \cdot 10^{-2}$	1.4	0.024

Table: Numerical results for Zalesak slotted cylinder after one revolution.

Numerical results: Zalesak slotted circle

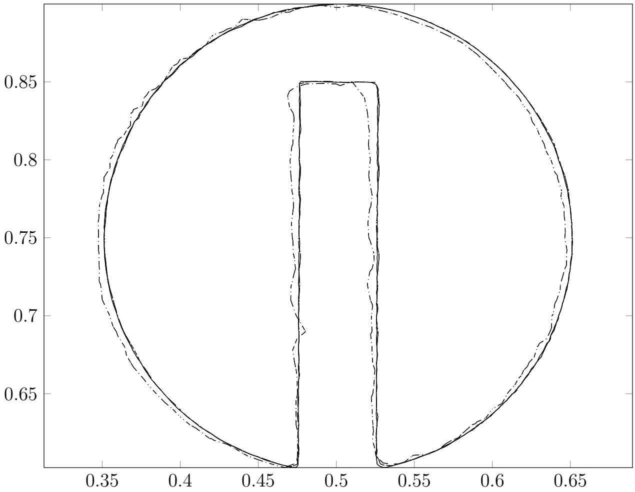

Figure: Numerical solution after 1 revolution

Outline

- This test illustrates the ability of the method to resolve thin filaments at scales of the mesh in stretching and tearing flows.
  - $\Gamma_0(0)$ is the boundary of a circle of radius 0.15 and center at $(0.5, 0.75)$.
  - Velocity field, $T = 8$

$$v_1(x_1, x_2) = -\sin^2(\pi x_1)\sin(2\pi x_2)\cos\left(\frac{\pi t}{T}\right),$$

$$v_2(x_1, x_2) = -\sin(2\pi x_1)\sin^2(\pi x_2)\cos\left(\frac{\pi t}{T}\right),$$

  - Numerical results

Meshes	n_p	Area loss	l^∞	L^1-order	l^∞-orde
M_1	$1.5 \cdot 10^4$	$3.53 \cdot 10^{-4}$	$1.457 \cdot 10^{-1}$	NA	NA
M_2	$1.5 \cdot 10^5$	$1.70 \cdot 10^{-4}$	$2.87 \cdot 10^{-2}$	1.04	2.34
M_3	$1.5 \cdot 10^6$	$2.58 \cdot 10^{-5}$	$1.42 \cdot 10^{-2}$	2.72	1.05

Table: Numerical results of the single vortex flow at time $T = 8$.

Numerical tests: Single vortex flow

- Comparison with other methods
  - Mesh: 128×128 and $T = 8$, L^1-norm $\int_D |u_{exac} - u_h| dx$

AMR-MOF	GPCA	Rider/Kothe	QMSL-PLS $(1.5 \cdot 10^3)$	QMSL-PLS $(1.5 \cdot 10^4)$
$5.04 \cdot 10^{-4}$	$1.17 \cdot 10^{-3}$	$1.44 \cdot 10^{-3}$	$5.22 \cdot 10^{-4}$	$1.88 \cdot 10^{-4}$

Table: L^1-norm errors at time $T = 8$.

- AMR-MOF: H. T. Ahn and M. Shashkov, *Adaptive moment-of-fluid method.* J. Comput. Phys. **228** (2009), pp. 2792-2821.
- GPCA: A. Cervone, S. Manservisi, R. Scardovelli and S. Zaleski, *A geometrical predictor-corrector advection scheme and its application to the volume fraction function.* J. Comput. Phys. **228** (2009), pp. 406-419.
- Rider/Kothe: W. J. Rider and D. B. Kothe, *Reconstructing volume tracking.* J. Comput. Phys. **141** (1998), pp. 112-152.

Numerical tests: Single vortex flow

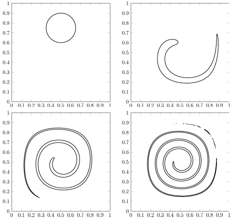

Figure: The numerical solution for the single vortex flow in mesh M_2 at time instants $t = 0$ (upper left panel), $t = 1$ (upper right panel), $t = 3$ (lower left panel) and $t = 5$ (lower right panel).

Outline

Numerical tests: The bubble rising

- The geometry of the rising bubble

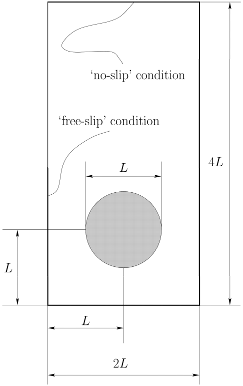

Figure: Geometry of the rising bubble problem. L is the characteristic length.

Numerical tests: The bubble rising

- Equations

$$\rho(u)\frac{Dv}{Dt}+\nabla p=\frac{1}{Re}\nabla\cdot(\mu(u)(\nabla v+(\nabla v)^T))+\frac{\rho(u)(-\mathbf{e}_2)}{Fr^2}+\frac{1}{We}\kappa(u)\delta(u)\mathbf{r}$$

$$\nabla\cdot v=0,$$

$$\frac{\partial u}{\partial t}+v\cdot\nabla u=0,$$

where δ is the Dirac function, κ denotes the dimensionless curvature, and *Re*, Fr^2 and *We* are dimensionless numbers.

Numerical tests: The bubble rising

- Boundary conditions: (1) $v = 0$ on the upper and lower boundaries, (2) free slip on lateral boundaries.
- Dimensionless numbers

$$Re = \frac{\rho_1 UL}{\mu_1}, \quad We = \frac{\rho_1 U^2 L}{\sigma}, \quad Fr = \frac{U^2}{gL}$$

  where $U = \sqrt{2gR}$ and $L = 2R$
- The coefficients

$$\rho(u) = \frac{\rho_2}{\rho_1} + (1 - \frac{\rho_2}{\rho_1})H_\eta(u), \quad \mu(u) = \frac{\mu_2}{\mu_1} + (1 - \frac{\mu_2}{\mu_1})H_\eta(u);$$

  ,
- the Heaviside graph

$$H_\eta(u) = \begin{cases} 0 \quad \text{if} \quad u < -\eta \\ \frac{1}{2}\left[1 + \frac{u}{\eta} + \frac{1}{\pi}\sin(\frac{\pi u}{\eta})\right]. \\ 1 \quad \text{if} \quad u > \eta. \end{cases}$$

Numerical tests: The bubble rising

Numerical solution method

- Space discretization
  - Taylor-Hood P_2/P_1 finite element for v and p and P_1-iso P_2 for the level set function
- Time discretization
  - BDF2-Modified Lagrange-Galerkin for the NS equations,
  - QMSL-PSL for the level set equations.

Numerical tests: The bubble rising

Physical parameters of the test

- Benchmark test 2 proposed by:
  S. Hysing, S. Turek, D. Kuzmin, N. Parolini, E. Burnman, S. Ganesan and L. Tobiska, *Proposal for quantitative benchmark computations of bubble dynamics.* Int. J. Numer. Meth. Fluids **60** (2009), pp. 1259-1288.

$$\rho_1 = 1000, \quad \rho_2 = 1, \quad \mu_1 = 10; \quad \mu_2 = 0.1, \quad g = 0.98,$$

$$Fr = 1, \quad \sigma = 1.96, \quad Re = 35, \quad We = 125.$$

Parameters of the numerical experiments:
$\Delta t = H/8$, $n_p = 1.5 \cdot 10^4$, $\eta = h$; β, r_{max} and r_{min} as in Zalesak slotted circle experiment.

Numerical tests: The bubble rising

Quantities to monitor the performance of the method

$$\mathbf{x}_{cog}(t) = (x_{1cog}(t), x_{2cog}(t) = \frac{\int_{D_2} \mathbf{x}(t)}{D_2}, \quad v_{2cog}(t) = \frac{dx_{2cog}}{dt},$$

$$circ(t) = \frac{P_a}{P_b}.$$

Results at different meshes

$1/H$	40	80	160
$circ_{\min}$	0.5222	0.5394	0.5334
$t\,(circ_{\min})$	2.4313	2.3003	2.3168
$v_{cog,\max 1}$	0.2586	0.2584	0.2579
$t\,(v_{cog,\max 1})$	0.6672	0.6566	0.6449
$v_{cog,\max 2}$	0.2495	0.2612	0.2558
$t\,(v_{cog,\max 2})$	1.9499	2.0078	2.0297
$y_{cog}(t=3)$	1.0950	1.1205	1.1195

Table: Minimum circularity and (both) maximum rise velocities, with corresponding times, and final position of center of gravity for test case2.

Numerical tests: The bubble rising

Comparison with the results of the methods of Hysing et al. paper

Group	TP2D	FREELIFE	MooNMD	QMSL-PLS
$circ_{\min}$	0.5869	0.4647	0.5114	0.5334
$t\,(circ_{\min})$	2.4004	3.0000	3.0000	2.3168
$v_{cog,\max 1}$	0.2524	0.2514	0.2502	0.2579
$t\,(v_{cog,\max 1})$	0.7332	0.7281	0.7317	0.6449
$v_{cog,\max 2}$	0.2434	0.2440	0.2393	0.2558
$t\,(v_{cog,\max 2})$	2.0705	1.9844	2.0600	2.0297
$y_{cog}(t=3)$	1.1380	1.1249	1.1376	1.1195

Table: Test quantities calculated by the following methods: TP2D with $H = 1/640$, FREELIFE with $H = 1/160$, MooNMD with $NDOF_{int} = 900$, and QMSL-PLS with $H = 1/160$.

Numerical tests: The bubble rising

Comparison with the results of the methods of Hysing et al. paper

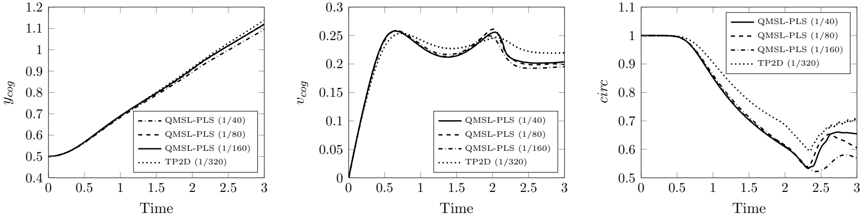

Figure: Graphics of y_{cog}, v_{cog}, $circ$ of the bubble.

Numerical tests: The bubble rising

Comparison with the results of the methods of Hysing et al. paper

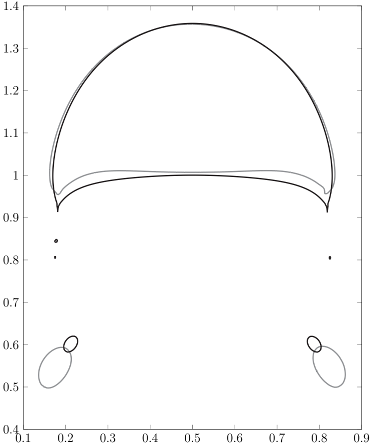

Figure: Shape of the bubble at $T = 3$. TP2D ($H = 1/320$) dark line, QMSL-PLS ($H = 1/160$) grey line .